

**Kaon pair production in proton-nucleus collisions at 2.83 GeV kinetic energy**

Yu. T. Kiselev,<sup>1,\*</sup> M. Hartmann,<sup>2,†</sup> A. Polyanskiy,<sup>1,2</sup> E. Ya. Paryev,<sup>1,3</sup> S. Barsov,<sup>4</sup> M. Büscher,<sup>5</sup> S. Dymov,<sup>2,6</sup> R. Gebel,<sup>2</sup> V. Hejny,<sup>2</sup> A. Kacharava,<sup>2</sup> I. Keshelashvili,<sup>2</sup> B. Lorentz,<sup>2</sup> Y. Maeda,<sup>7</sup> S. Merzliakov,<sup>2,6</sup> S. Mikirtychiants,<sup>2,4</sup> H. Ohm,<sup>2</sup> V. Serdyuk,<sup>2,6</sup> A. Sibirtsev,<sup>8,‡</sup> V. Y. Sinityna,<sup>9</sup> H. J. Stein,<sup>2</sup> H. Ströher,<sup>2</sup> S. Trusov,<sup>10,11</sup> Yu. Valdau,<sup>4,12</sup> C. Wilkin,<sup>13</sup> P. Wüstner,<sup>14</sup> and Q. J. Ye<sup>2,15</sup>

<sup>1</sup>*Institute for Theoretical and Experimental Physics, RU-117218 Moscow, Russia*

<sup>2</sup>*Institut für Kernphysik, Forschungszentrum Jülich, D-52425 Jülich, Germany*

<sup>3</sup>*Institute for Nuclear Research, Russian Academy of Sciences, RU-117312 Moscow, Russia*

<sup>4</sup>*High Energy Physics Department, Petersburg Nuclear Physics Institute, RU-188350 Gatchina, Russia*

<sup>5</sup>*Peter Grünberg Institut (PGI-6), Forschungszentrum Jülich, D-52425 Jülich, Germany*

<sup>6</sup>*Laboratory of Nuclear Problems, Joint Institute for Nuclear Research, RU-141980 Dubna, Russia*

<sup>7</sup>*Research Center for Nuclear Physics, Osaka University, Ibaraki, Osaka 567-0047, Japan*

<sup>8</sup>*Department of Physics and Astronomy, University of Manitoba, Winnipeg, Manitoba R3T 2N2, Canada*

<sup>9</sup>*P. N. Lebedev Physical Institute, RU-119991 Moscow, Russia*

<sup>10</sup>*Institut für Kern- und Hadronenphysik, Helmholtz-Zentrum Dresden-Rossendorf, D-01314 Dresden, Germany*

<sup>11</sup>*Skobeltsyn Institute of Nuclear Physics, Lomonosov Moscow State University, RU-119991 Moscow, Russia*

<sup>12</sup>*Helmholtz-Institut für Strahlen- und Kernphysik, Universität Bonn, D-53115 Bonn, Germany*

<sup>13</sup>*Physics and Astronomy Department, UCL, London WC1E 6BT, United Kingdom*

<sup>14</sup>*Zentralinstitut für Elektronik, Forschungszentrum Jülich, D-52425 Jülich, Germany*

<sup>15</sup>*Department of Physics and Triangle Universities Nuclear Laboratory, Duke University, Durham, North Carolina 27708, USA*

(Received 9 September 2015; published 3 December 2015)

The production of non- $\phi K^+ K^-$  pairs by protons at 2.83 GeV kinetic energy on C, Cu, Ag, and Au targets has been investigated by using the COSY-ANKE magnetic spectrometer. The  $K^-$  momentum dependence of the differential cross section has been measured for laboratory polar angles  $\theta_{K^\pm} \leq 12^\circ$  over the 0.2–0.9 GeV/c range. The comparison of the data with detailed model calculations indicates an attractive  $K^-$ -nucleus potential of about  $-60$  MeV at normal nuclear matter density at a mean momentum of 0.5 GeV/c. However, this approach has difficulty in reproducing the smallness of the observed cross sections at low- $K^-$  momenta.

DOI: [10.1103/PhysRevC.92.065201](https://doi.org/10.1103/PhysRevC.92.065201)

PACS number(s): 13.75.-n, 14.40.Be, 25.40.-h

**I. INTRODUCTION**

The study of kaon and antikaon properties in a strongly interacting environment has been a very active research field over the last two decades (see, e.g., Refs. [1–3]), especially in connection with questions of the partial restoration of chiral symmetry in hot or dense nuclear matter and of the existence of a  $K^-$  condensate in neutron stars.

It is reasonably well established [1–3] that the  $K^+$  meson feels a moderately repulsive nuclear potential of about 20–30 MeV at normal nuclear matter density,  $\rho_0 = 0.16 \text{ fm}^{-3}$ . In contrast, the properties of the  $K^-$  meson in nuclear matter are still the subject of very intense debate. This is due to the complicated dynamics of antikaons inside nuclei, which lead to modifications of their in-medium properties. These require complex self-consistent coupled-channel calculations, with the inclusion of complete sets of pseudoscalar meson and baryon octets. Such calculations, based on chiral Lagrangians [4–10] or on meson-exchange potentials [11,12], predict relatively shallow low-energy  $K^-$ -nucleus potentials with central depths of the order of  $-50$  to  $-80$  MeV. On the other hand, fits to

the  $K^-$  atomic data [13,14], in terms of phenomenological density-dependent optical potentials or relativistic mean-field calculations [15], lead to much stronger potentials with depths of about  $-200$  MeV at density  $\rho_0$ . This is in line with the results obtained in one experiment [16,17] but is in conflict with the self-consistent approaches mentioned above. However, it should be noted that the antikaonic-atom data probe the surface of the nucleus and thus do not provide strong constraints on the  $K^-$ -nucleus potential at normal nuclear matter density.

Motivated by the idea that a very strong antikaon-nucleon potential could lead to deeply bound kaonic states [18,19], many experiments [20–31] have been performed to search for them. Some experiments claim positive signals [20–25,31] while others do not [26–30]. The Valencia theory group has argued that, at present, there is no firm experimental evidence for either the existence of deeply bound kaonic states or for a strong antikaon-nucleus potential [32–35].

Information about in-medium properties of antikaons can be deduced also from the study of their production in both heavy-ion and proton-nucleus collisions at incident energies near or below the free nucleon-nucleon threshold (2.5 GeV). This can be understood within a scenario where a reduction of the  $K^-$  mass inside the nucleus would lead to an enhancement of the  $K^-$  yield in these collisions, due to in-medium shifts of the elementary production thresholds to lower energies.

\*yurikis@itep.ru

†m.hartmann@fz-juelich.de

‡Deceased.

However, it was shown [1,3] that the existence of a  $K^-$  condensate is not compatible with the available heavy-ion data.

The KaoS data [36] on the ratio of  $K^-$  and  $K^+$  inclusive momentum spectra from reactions  $p + A \rightarrow K^\pm + X$  with  $A = C$  and Au at laboratory angles from  $36^\circ$  to  $60^\circ$  and beam energy of 2.5 GeV have been analyzed within the Boltzmann–Uehling–Uhlenbeck (BUU) transport model [36]. These calculations have shown that the data are consistent with an in-medium  $K^-A$  potential of the order of  $-80$  MeV at normal nuclear density. This is in agreement with an antikaon attraction of  $-110 \pm 10$  MeV extracted from heavy-ion data [37,38].

There were measurements at the Institute for Theoretical and Experimental Physics (ITEP) accelerator of inclusive antikaon momentum distributions from 0.6 to 1.3 GeV/ $c$  at a laboratory angle of  $10.5^\circ$  in  $p\text{Be}$  and  $p\text{Cu}$  interactions at 2.25 and 2.4 GeV beam energies [39,40]. The  $K^-$  excitation functions in these interactions were also determined for a  $K^-$  momentum of 1.28 GeV/ $c$  at bombarding energies  $<3$  GeV. A reasonable description of these data was achieved in the framework of a folding model, based on the target nucleon momentum distribution and on free elementary cross sections, assuming vacuum  $K^+$  and  $K^-$  masses [39,40]. A  $K^-$  potential of about  $-28$  MeV at density  $\rho_0$  at a momentum of 800 MeV/ $c$  has been extracted [41] from data on elastic  $K^-A$  scattering within Glauber theory.

Given the diverse results, one must admit that the situation with regards to the antikaon-nucleus optical potential is still very unclear. To make progress in understanding the strength of the  $K^-$  interaction in the nuclear medium, it is necessary to carry out detailed measurements with tagged low-momentum  $K^-$  mesons. These must not stem from  $\phi$  decays so that they bring “genuine” information about this strength. Such measurements were recently performed by the Apparatus for Studies of Nucleon and Kaon Ejectiles (ANKE) Collaboration at the Cooler Synchrotron (COSY) of the Forschungszentrum Jülich, where the production of  $K^+K^-$  pairs with invariant masses corresponding to both the  $\phi$  and non- $\phi$  regions was studied in proton collisions with C, Cu, Ag, and Au targets at an incident beam energy of 2.83 GeV [42,43]. These data allowed the momentum dependence of the  $\phi$  nuclear transparency ratio, the in-medium  $\phi$  meson width, and the differential cross section for its production at forward angles to be determined for these targets over the  $\phi$  momentum range of 0.6–1.6 GeV/ $c$  [42,43].

An analysis is here presented of the data from the non- $\phi$  region of invariant masses, where differential cross sections for  $K^+K^-$  pair production on the four targets were obtained as functions of the  $K^-$  laboratory momentum. Results of this analysis are compared with model calculations, based on the nuclear spectral function for incoherent primary proton-nucleon and secondary pion-nucleon  $K^+K^-$  creation processes within different scenarios for the  $K^-$  nuclear potential [44].

## II. EXPERIMENT AND RESULTS

The experiment was performed at the COSY [45] by using the ANKE magnetic spectrometer [46,47] that is located at an internal target station of the storage ring. ANKE contains three

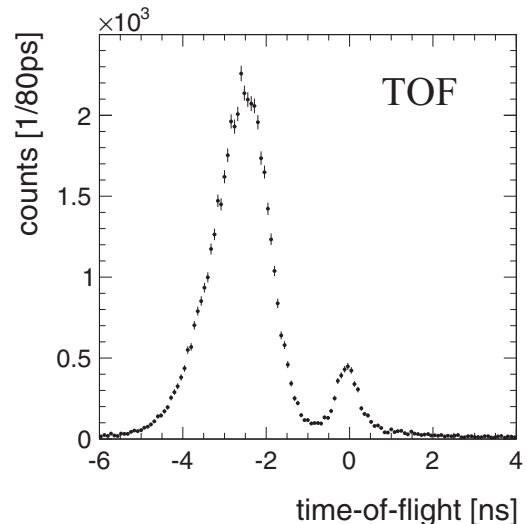


FIG. 1. Time-of-flight difference between the stop counters in the negative and positive detection systems for the carbon target. The left and right peaks contain the  $K^+\pi^-$  and  $K^+K^-$  events, respectively.

dipole magnets; D1 and D3 divert the circulating beam onto the target and back into the COSY ring, respectively, while D2 is the analyzing magnet. A series of thin and narrow C, Cu, Ag, and Au targets was inserted in a circulating beam of 2.83 GeV protons in front of the main spectrometer magnet D2. The ANKE spectrometer has detection systems placed to the right and left of the beam to register positively and negatively charged ejectiles which, in the case of nonresonant kaon pair production, are the  $K^+$  and  $K^-$ . Although only used here for efficiency studies, forward-going charged particles could also be measured in coincidence.

The positively charged kaons were first selected by using a dedicated detection system that can identify a  $K^+$  against a pion and/or proton background that is  $10^5$  times more intense [48–50]. The  $K^-$  mesons in correlation with the  $K^+$  were subsequently identified from the time-of-flight difference between stop counters in the negative and positive detection systems. Figure 1 shows a distribution of such overall time differences between the negative and positive stop counters for the carbon target after correcting for the time delays among different counters, using information derived from the particle momenta [47,49,50].

The peak around zero corresponds to  $K^+K^-$  pairs and this sits on a small background of misidentified particles. The large peak at negative time differences stems from negative pions, which are faster than the  $K^-$  mesons but are still in coincidence with the  $K^+$  mesons registered in the positive detector. A  $3\sigma$  cut around the right peak was made to select the  $K^+K^-$  events. This part of the spectrum is also used to estimate the residual background for the kaon pairs. The background for the heavier targets of Cu, Ag, and Au is noticeably smaller than that for C.

The resulting invariant mass spectrum of the selected  $K^+K^-$  pairs for C is given in Fig. 2. One can see that there is a strong  $\phi$  signal that sits on a broad distribution of non- $\phi$  kaon pair production. The invariant mass spectra for Cu, Ag, and Au look similar to that for C [42,43,50]. To separate the nonresonant kaon pair production events from

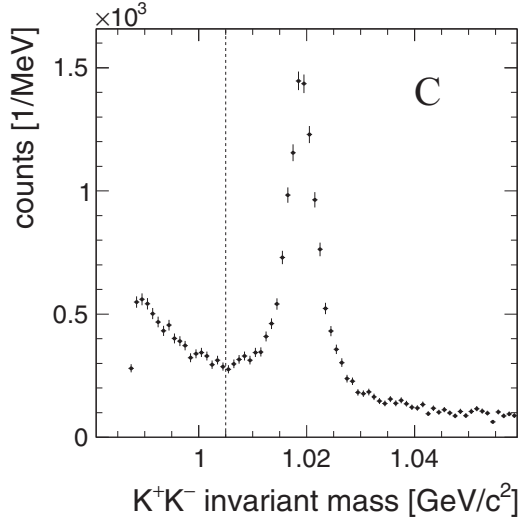


FIG. 2. Invariant mass ( $IM$ ) distribution for  $K^+K^-$  pairs produced in  $p$ -C collisions at 2.83 GeV beam energy. The vertical line indicates the cut  $IM \leq 1.005$  GeV/ $c^2$  used for the separation of the non- $\phi$  and  $\phi$ -rich regions.

those arising from the decay of the strong  $\phi$  resonance, a cut on the invariant mass of the  $K^+K^-$  pairs,  $IM \leq 1.005$  GeV/ $c^2$ , was applied in the subsequent analysis. The initial proton kinetic energy of 2.83 GeV corresponds to an excess energy of 108 MeV above the threshold for kaon pair creation in proton-nucleon collisions. The accessible ranges of the  $K^+$  and  $K^-$  meson momenta were  $0.2$  GeV/ $c \leq p_{K^+} \leq 0.6$  GeV/ $c$  and  $0.2$  GeV/ $c \leq p_{K^-} \leq 0.9$  GeV/ $c$ , respectively. The polar production angle was restricted to  $12^\circ$  for both positively and negatively charged kaons.

In order to evaluate the double-differential cross section for nonresonant ( $IM \leq 1.005$  GeV/ $c^2$ )  $K^+K^-$  production in  $pA$  collisions, the  $K^-$  momentum range was divided into six bins. The numbers  $N_{K^+K^-}^A$  of kaon pairs with the  $K^-$  in a momentum bin of width  $\Delta p_{K^-}$  and solid angle  $\Delta\Omega_{K^-}$  in coincidence with a  $K^+$  meson with momentum  $0.2$  GeV/ $c \leq p_{K^+} \leq 0.6$  GeV/ $c$  and detected in solid angle  $\Delta\Omega_{K^+}$  were determined for the four

targets. The cross section was then evaluated from

$$\frac{d^2\sigma_{pA \rightarrow K^+K^-X}}{(dp d\Omega)_{K^+}(dp d\Omega)_{K^-}} = \frac{1}{(\Delta p_{K^+} \Delta\Omega_{K^+})(\Delta p_{K^-} \Delta\Omega_{K^-})} \times \frac{N_{K^+K^-}^A}{\langle \epsilon_{K^+K^-} \rangle L_{\text{int}}^A}, \quad (1)$$

where  $\Delta p_{K^+} = 0.4$  GeV/ $c$ ,  $\Delta\Omega_{K^\pm} = 2\pi(1 - \cos 12^\circ)$  and  $L_{\text{int}}^A$  is the integrated luminosity for target  $A$ .

In order to estimate the average efficiency for  $K^+K^-$  identification ( $\epsilon_{K^+K^-}$ ), the detection efficiency was first evaluated for each nucleus and each  $K^-$  momentum bin. For this purpose the number of  $K^+K^-$  pairs detected relative to that determined from fitting the  $K^+K^-$  efficiency-corrected absolute time-of-flight distributions was calculated on an event-by-event basis. These efficiencies were then averaged over the target nuclei for each momentum bin. The root-mean-square deviations of the individual efficiencies from the  $\langle \epsilon_{K^+K^-} \rangle$  mean were about 5%, which is consistent with the statistical precision.

The overall efficiency was estimated for each event as the product of the individual efficiencies:

$$\epsilon_{K^+K^-} = \epsilon_{\text{tel}} \epsilon_{\text{tr}} \epsilon_{\text{acc}}. \quad (2)$$

The track reconstruction efficiency of  $K^+K^-$  pairs  $\epsilon_{\text{tr}}$  was determined from the experimental data. The correction for kaon decay in flight and acceptance,  $\epsilon_{\text{acc}}$ , was estimated as a function of the laboratory momenta and polar angles of kaons, by using simulations. The range-telescope efficiency  $\epsilon_{\text{tel}}$  was extracted from calibration data on  $K^+p$  coincidences. The integrated luminosity  $L_{\text{int}}^A$  was calculated by using the measured flux of  $\pi^+$  mesons with momenta  $\approx 500$  MeV/ $c$  produced at small laboratory angles [51].

The statistical uncertainties were about 7% for each momentum bin and nucleus. The overall systematic uncertainties were typically 14%, rising to 16% for the first and last momentum bins. The main sources of the systematic effects are related to the simulation of acceptance corrections  $\epsilon_{\text{acc}}$  (5%–10%), the determination of the range-telescope efficiency  $\epsilon_{\text{tel}}$  (10%), and the estimation of the integrated luminosity  $L_{\text{int}}^A$  (8%).

The measured double-differential cross sections for nonresonant  $K^+K^-$  pair production are given in Table I for the

TABLE I. The measured double-differential cross sections  $d^2\sigma_{pA \rightarrow K^+K^-X}/(dp d\Omega)_{K^+}(dp d\Omega)_{K^-}$  [in  $\mu\text{b}/(\text{GeV}/c)^2\text{sr}^2$ ] of Eq. (1) for nonresonant  $K^+K^-$  production in the interaction of 2.83 GeV protons with C, Cu, Ag, and Au target nuclei. The data, which are averaged over small kaon angles,  $\theta_{K^\pm} \leq 12^\circ$ , and over  $K^+$  momenta in the range  $200 \leq p_{K^+} \leq 600$  MeV/ $c$ , are presented in bins of  $K^-$  momenta. The first errors are statistical and the second systematic, which are associated with the background subtraction and include the uncertainty in the average detection efficiency  $\epsilon_{K^+K^-}$ . There are in addition overall systematic uncertainties that are discussed in the text. The last line shows the cross sections [in  $\mu\text{b}/(\text{GeV}/c)\text{sr}^2$ ] integrated over the total measured  $K^-$  momentum range. The related uncertainties are compounds of the statistical and systematic errors.

$p_{K^-}$ [MeV/ $c$ ]	C	Cu	Ag	Au
200–350	$2.7 \pm 0.2 \pm 0.4$	$6.2 \pm 0.6 \pm 0.8$	$6.5 \pm 0.8 \pm 0.7$	$11.7 \pm 1.1 \pm 1.2$
350–450	$8.1 \pm 0.5 \pm 0.8$	$18.6 \pm 1.2 \pm 1.7$	$26.2 \pm 1.8 \pm 2.4$	$33.1 \pm 2.2 \pm 3.1$
450–550	$12.7 \pm 0.6 \pm 0.8$	$27.8 \pm 1.6 \pm 1.6$	$32.2 \pm 2.2 \pm 1.9$	$41.7 \pm 2.8 \pm 2.4$
550–650	$11.9 \pm 0.6 \pm 0.8$	$19.3 \pm 1.4 \pm 1.3$	$29.7 \pm 2.1 \pm 2.1$	$30.5 \pm 2.6 \pm 2.2$
650–750	$6.6 \pm 0.5 \pm 0.4$	$12.3 \pm 1.2 \pm 0.8$	$13.5 \pm 1.6 \pm 0.6$	$18.4 \pm 2.1 \pm 2.7$
750–900	$2.5 \pm 0.3 \pm 0.6$	$3.4 \pm 0.7 \pm 0.8$	$4.4 \pm 1.0 \pm 1.2$	$6.3 \pm 1.4 \pm 1.7$
200–900	$4.7 \pm 0.2$	$9.5 \pm 0.5$	$11.8 \pm 0.6$	$15.1 \pm 0.8$

four targets. The overall systematic uncertainties of these cross sections have not been included.

### III. ANALYSIS OF DATA

Figure 3 shows the measured double-differential cross sections for  $K^+K^-$  production off C, Cu, Ag, and Au targets compared to calculations within the collision model based on the nuclear spectral function for incoherent primary proton-nucleon and secondary pion-nucleon pair-creation processes [44]. The model includes initial proton and final kaon absorption, using the free  $pN$  and  $KN$  cross sections, target nucleon binding, and Fermi motion, as well as nuclear mean-field-potential effects. The calculations, which take into account the ANKE acceptance, were performed assuming four options for the  $K^-$  nuclear potential depth  $U$  at nuclear matter density  $\rho_0 = 0.16 \text{ fm}^{-3}$ , viz.  $U = 0 \text{ MeV}$ ,  $U = -60 \text{ MeV}$ ,  $U = -126 \text{ MeV}$ , and  $U = -180 \text{ MeV}$ .

It is seen from the figure that, in general, the calculated cross sections for  $K^-$  potential depths  $U = -60, -126,$  and  $-180 \text{ MeV}$  follow the data for all target nuclei for laboratory antikaon momenta above about  $0.4 \text{ GeV}/c$ ; the data exclude the possibility of weak nuclear antikaon mass shifts. The measured double-differential cross sections on light C and medium Cu targets are better reproduced at these momenta by the model calculations with a stronger  $K^-$  potential. For heavy Ag

and Au nuclei the comparison of data and calculations favors the weaker antikaon potential. On the other hand, the data at lower antikaon momenta are reproduced reasonably well with almost no  $K^-$  potential and are overestimated by all the calculation with a nonzero antikaon potential. This suggests that the model misses some peculiarities of the absorption of low-momentum  $K^-$  mesons and/or their production in nuclear matter.

In the following analysis of the data, aiming at the determination of the real part of the antikaon nuclear potential at saturation density, we make use of the cross sections integrated over the measured  $K^-$  momentum interval, i.e., on the last line of Table 1, rather than on the differential ones shown in Fig. 3. Due to the increased number of counts, this approach has the advantage of decreasing significantly the statistical uncertainties to less than about 3%. In addition, the errors associated with the background subtraction decrease to about 4%. This approach also leads to a decrease of the overall systematic uncertainties. Evidently, the antikaon potential depth extracted in this way will correspond to an average  $K^-$  momentum of about  $0.5 \text{ GeV}/c$ , in the vicinity of which the main strength of the measured distributions is concentrated. The target mass dependence of the integrated cross sections follows the power law  $A^\alpha$  with the exponent  $\alpha_{K^+K^-} = 0.42 \pm 0.02$ , which is less than  $\alpha_\phi = 0.56 \pm 0.03$  for the  $\phi$  mesons [42].

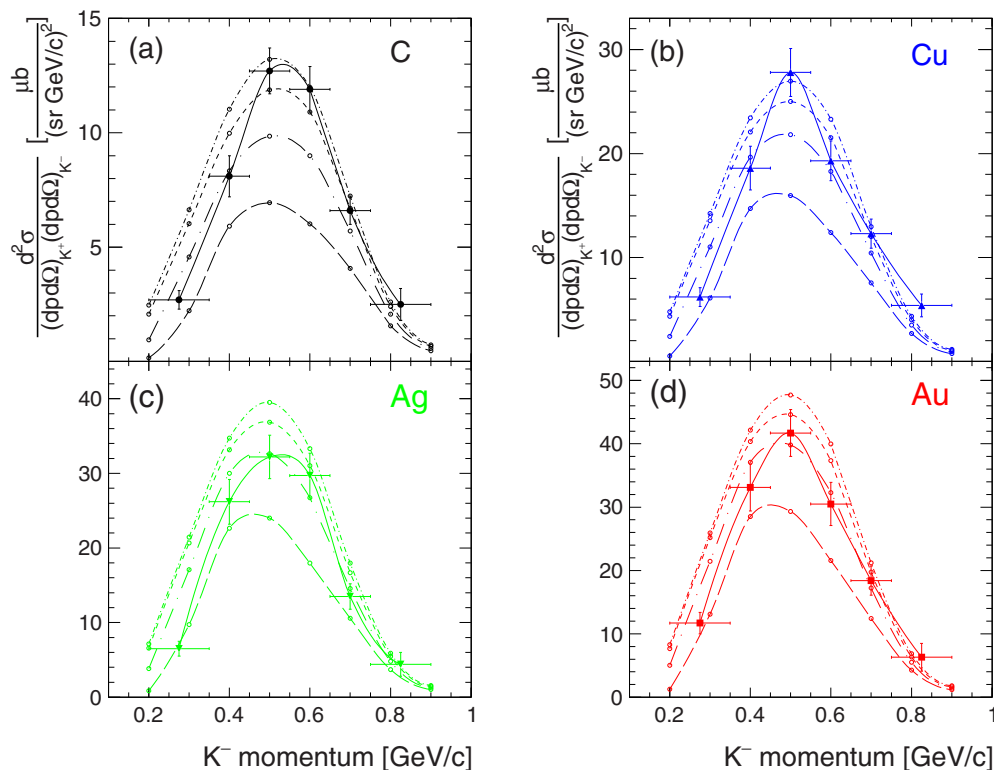


FIG. 3. (Color online) Double-differential cross sections for the production of nonresonant  $K^+K^-$  pairs in the ANKE acceptance in the collisions of  $2.83 \text{ GeV}$  protons with (a) C, (b) Cu, (c) Ag, and (d) Au targets as functions of the  $K^-$  laboratory momentum. The experimental data, which are taken from from Table I, are averaged over small kaon angles,  $\theta_{K^\pm} \leq 12^\circ$ , and over  $K^+$  momenta in the range  $200 \leq p_{K^+} \leq 600 \text{ MeV}/c$ . The curves represent, from the bottom to top, model calculations [44] for  $K^-$  potential depths  $U = 0 \text{ MeV}$  (long dashed),  $-60 \text{ MeV}$  (dot long dashed),  $-126 \text{ MeV}$  (short dashed), and  $-180 \text{ MeV}$  (dot short dashed), respectively. The solid lines are simple spline functions through the experimental data points.

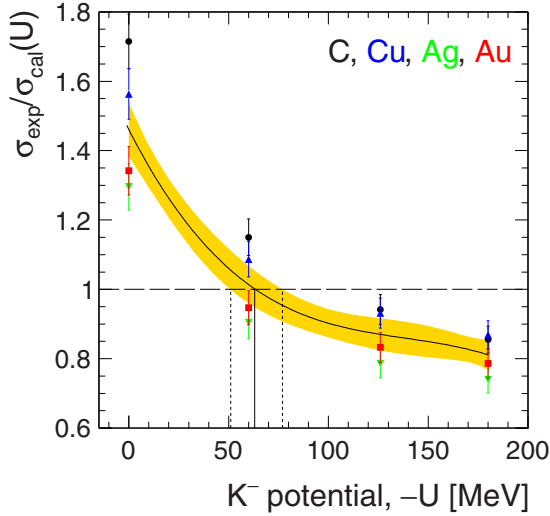


FIG. 4. (Color online) Ratio of the measured integrated cross section for nonresonant  $K^+K^-$  pair production on a given nucleus  $A$  to the corresponding cross sections, calculated within the adopted model and supposing four values for the  $K^-$  potential depth at nuclear matter density:  $U = 0$  MeV,  $-60$  MeV,  $-126$  MeV, and  $-180$  MeV. The curve represents a third-order polynomial fit of all ratios presented in the figure, with the shaded band indicating the  $1\sigma$  confidence interval. The pair of vertical dotted lines corresponds to the regions where the ratio is unity within the errors given by the third-order fit. The color code is identical to that shown explicitly in Fig. 3.

To determine the  $K^-$  nuclear potential, we consider the ratio of the measured integrated cross section for the nonresonant  $K^+K^-$  pair production on a given nucleus  $A$ , as presented in the last line of Table 1, to the corresponding cross sections calculated within the model for different potential strengths. The values of  $\sigma_{\text{exp}}/\sigma_{\text{cal}}(U)$  are shown in Fig. 4 for  $U = 0$  MeV,  $U = -60$  MeV,  $U = -126$  MeV, and  $U = -180$  MeV. Also shown is a third-order polynomial fit to the complete data set of ratios.

It is seen from the figure that the condition that  $\sigma_{\text{exp}}/\sigma_{\text{cal}} = 1$  is achieved if  $U = -(63_{-12}^{+15})$  MeV. However, this estimate does not include the overall systematic uncertainty in the data. The calculations have therefore been repeated with the cross sections increased or decreased by a 13% uncertainty. This leads to the much-expanded error band of  $U = -(63_{-31}^{+50})$  MeV. The width of this band could only be reduced by controlling better the systematic uncertainties in the values of the cross sections.

Within the uncertainties quoted, the value obtained for the potential depth is consistent with the moderate  $K^-$ -nucleus potential of the order of  $-50$  to  $-80$  MeV that is predicted by calculations based on chiral Lagrangians [4–10] or on meson-exchange potentials [11,12]. It also agrees with the potential of the order of  $-80$  MeV at normal nuclear density extracted from KaoS  $pA$  data [36], as well as with a lower potential of about  $-28$  MeV at saturation density extracted at an antikaon momentum of  $800$  MeV/ $c$  [41]. However, it is hard to reconcile our value with the deep potential of order  $-200$  MeV claimed

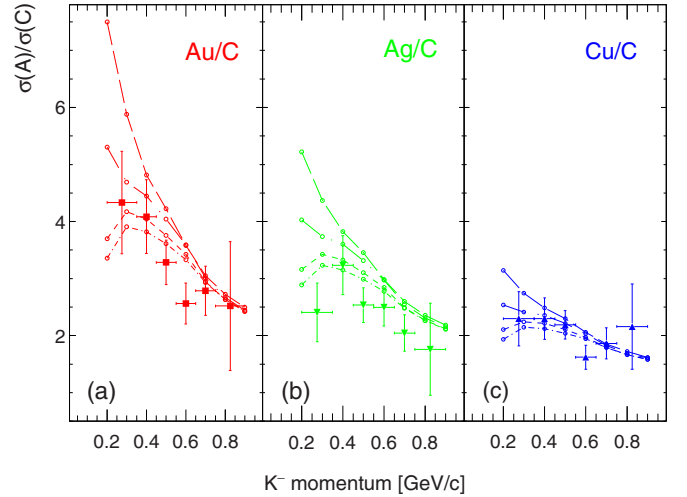


FIG. 5. (Color online) Ratios of the measured and calculated double-differential cross sections for nonresonant  $K^+K^-$  pair production off (a) Au, (b) Ag, and (c) Cu targets presented in Fig. 3, to the measured and calculated ones for the C target, given also in the same figure as functions of the  $K^-$  laboratory momentum. The color code and the notation of the curves are the same as those in Fig. 3.

in experiments that studied in-flight  $(K^-, N)$  reactions on  $^{12}\text{C}$  and  $^{16}\text{O}$  at  $1$  GeV/ $c$  [16,17]. On the other hand, it has been argued [52,53] that the  $(K^-, N)$  experiment was not suitable for extracting information on the depth of the  $K^-$ -nucleus optical potential, although it could provide valuable information about two- and three-nucleon-absorption mechanisms.

Finally, in Fig. 5 we show the ratios of the measured and calculated double-differential cross sections for nonresonant  $K^+K^-$  production off Cu, Ag, and Au targets to the same for a C target, as functions of the  $K^-$  laboratory momentum. It is worth mentioning that cross-section ratios can be determined with less ambiguity than cross sections themselves, since the normalization and detector-dependent uncertainties, as well as theoretical uncertainties associated with the particle production and absorption mechanisms, largely cancel out. On the other hand, apart from the sensitivity to the particle absorption in nuclear medium, which is determined by the imaginary part of particle nuclear potential, such ratios also reveal some sensitivity to the real part of this potential at low momenta (cf. Fig. 5). The comparison of the strengths and shapes of the data and calculations provides evidence for a moderately attractive antikaon optical potential for all the  $K^-$  momenta studied. This is in line with our findings based on the analysis of the integrated cross sections. However, due to the large errors in the ratios shown in Fig. 5, these data do not allow one to get definitive information about the value of this potential.

#### IV. CONCLUSIONS

We measured the differential cross sections for nonresonant  $K^+K^-$  pair production on carbon, copper, silver, and gold targets by  $2.83$  GeV protons with the ANKE magnetic spectrometer over the antikaon momentum range of  $0.2$ – $0.9$  GeV/ $c$ .

In order to determine the  $K^-$  nuclear optical potential we have used a sample of data that is essentially free from contributions from the strong  $\phi$  meson resonance. Information on the depth of the antikaon nuclear potential was obtained by comparing the measured cross sections of the nonresonant  $K^+K^-$  pair production with calculations in the framework of a collision model that takes the ANKE acceptance of Eq. (1) into account. It is based on the nuclear spectral function for incoherent primary proton-nucleon and secondary pion-nucleon creation processes. Within the model used, the real part of the attractive  $K^-$  nuclear optical potential was found to be about  $-60$  MeV at normal nuclear density and mean  $K^-$  momentum of  $0.5$  GeV/ $c$ . Although the error bars are significant, it does

not favor a very deep antikaon potential at this momentum. Further theoretical efforts are needed to reliably describe the present ANKE data and, hence, to fully elucidate the antikaon dynamics in the nuclear matter, especially at low momenta.

#### ACKNOWLEDGMENTS

Support from other members of the ANKE Collaboration, as well as the COSY machine crew, are gratefully acknowledged. We are particularly appreciative of the encouragement that we received from Eulogio Oset. This work has been partially financed by the COSY FFE, the DFG, and the Ministry of Education and Science of the Russian Federation.

- 
- [1] W. Cassing and E. L. Bratkovskaya, *Phys. Rep.* **308**, 65 (1999).  
 [2] E. Friedman and A. Gal, *Phys. Rep.* **452**, 89 (2007).  
 [3] C. Hartnack *et al.*, *Phys. Rep.* **510**, 119 (2012).  
 [4] M. Lutz, *Phys. Lett. B* **426**, 12 (1998).  
 [5] J. Schaffner-Bielich, V. Koch, and M. Effenberger, *Nucl. Phys. A* **669**, 153 (2000).  
 [6] A. Ramos and E. Oset, *Nucl. Phys. A* **671**, 481 (2000).  
 [7] A. Cieply *et al.*, *Nucl. Phys. A* **696**, 173 (2001).  
 [8] A. Ramos *et al.*, *Nucl. Phys. A* **691**, 258 (2001).  
 [9] L. Tolos, A. Ramos, and E. Oset, *Phys. Rev. C* **74**, 015203 (2006).  
 [10] L. Tolos, D. Cabrera, and A. Ramos, *Phys. Rev. C* **78**, 045205 (2008).  
 [11] L. Tolos, A. Ramos, A. Polls, and T. T. S. Kuo, *Nucl. Phys. A* **690**, 547 (2001).  
 [12] L. Tolos, A. Ramos, and A. Polls, *Phys. Rev. C* **65**, 054907 (2002).  
 [13] E. Friedman, A. Gal, and C. J. Batty, *Phys. Lett. B* **308**, 6 (1993).  
 [14] E. Friedman, A. Gal, and C. J. Batty, *Nucl. Phys. A* **579**, 518 (1994).  
 [15] E. Friedman, A. Gal, J. Mares, and A. Cieply, *Phys. Rev. C* **60**, 024314 (1999).  
 [16] T. Kishimoto *et al.*, *Prog. Theor. Phys.* **118**, 181 (2007).  
 [17] T. Kishimoto *et al.*, *Nucl. Phys. A* **827**, 321c (2009).  
 [18] Y. Akaishi and T. Yamazaki, *Phys. Rev. C* **65**, 044005 (2002).  
 [19] Y. Akaishi, A. Dote, and T. Yamazaki, *Phys. Lett. B* **613**, 140 (2005).  
 [20] T. Suzuki *et al.*, *Phys. Lett. B* **597**, 263 (2004).  
 [21] T. Suzuki *et al.*, *Nucl. Phys. A* **754**, 375c (2005).  
 [22] M. Agnello *et al.*, *Phys. Rev. Lett.* **94**, 212303 (2005).  
 [23] M. Agnello *et al.*, *Nucl. Phys. A* **775**, 35 (2006).  
 [24] M. Agnello *et al.*, *Phys. Lett. B* **654**, 80 (2007).  
 [25] T. Yamazaki *et al.*, *Phys. Rev. Lett.* **104**, 132502 (2010).  
 [26] L. Fabbietti *et al.*, *Nucl. Phys. A* **914**, 60 (2013).  
 [27] E. Epple and L. Fabbietti, *Phys. Rev. C* **92**, 044002 (2015).  
 [28] G. Agakishiev *et al.*, *Phys. Lett. B* **742**, 242 (2015).  
 [29] M. Sato *et al.*, *Phys. Lett. B* **659**, 107 (2008).  
 [30] T. Hashimoto *et al.*, *Prog. Theor. Exp. Phys.* 061D01 (2015).  
 [31] Y. Ichikawa *et al.*, *Prog. Theor. Exp. Phys.* 021D01 (2015).  
 [32] E. Oset and H. Toki, *Phys. Rev. C* **74**, 015207 (2006).  
 [33] A. Ramos, V. K. Magas, E. Oset, and H. Toki, *Eur. Phys. J. A* **31**, 684 (2007).  
 [34] V. K. Magas, E. Oset, and A. Ramos, *Phys. Rev. C* **77**, 065210 (2008).  
 [35] V. K. Magas, A. Ramos, J. Yamagata-Sekihara, S. Hirenzaki, and E. Oset, *Nonlin. Phenom. Complex Syst.* **12**, 414 (2009).  
 [36] W. Scheinast *et al.*, *Phys. Rev. Lett.* **96**, 072301 (2006).  
 [37] W. Cassing *et al.*, *Nucl. Phys. A* **614**, 415 (1997).  
 [38] A. Sibirtsev and W. Cassing, *Nucl. Phys. A* **641**, 476 (1998).  
 [39] A. V. Akhondinov *et al.*, *JETP Lett.* **85**, 142 (2007).  
 [40] A. V. Akhondinov *et al.*, *J. Phys. G* **37**, 015107 (2010).  
 [41] A. Sibirtsev and W. Cassing, *arXiv:nucl-th/9909053*.  
 [42] A. Polyanskiy *et al.*, *Phys. Lett. B* **695**, 74 (2011).  
 [43] M. Hartmann *et al.*, *Phys. Rev. C* **85**, 035206 (2012).  
 [44] E. Ya. Paryev, M. Hartmann, and Yu. T. Kiselev, *J. Phys. G* **42**, 075107 (2015).  
 [45] R. Maier *et al.*, *Nucl. Instrum. Methods Phys. Res., Sect. A* **390**, 1 (1997).  
 [46] S. Barsov *et al.*, *Nucl. Instrum. Methods Phys. Res., Sect. A* **462**, 364 (2001).  
 [47] M. Hartmann *et al.*, *Int. J. Mod. Phys. A* **22**, 317 (2007).  
 [48] M. Büscher *et al.*, *Nucl. Instrum. Methods Phys. Res., Sect. A* **481**, 378 (2002).  
 [49] M. Hartmann *et al.*, *AIP Conf. Proc.* **1322**, 349 (2010).  
 [50] A. Polyanskiy *et al.*, *Yad. Fiz.* **75**, 100 (2012) [*Phys. At. Nucl.* **75**, 63 (2012)].  
 [51] M. Büscher *et al.*, *Eur. Phys. J. A* **22**, 301 (2004).  
 [52] V. K. Magas *et al.*, *Phys. Rev. C* **81**, 024609 (2010).  
 [53] A. Ramos *et al.*, *Nucl. Phys. A* **835**, 382 (2010).